RESEARCH ARTICLE

Analysis of Doppler and Multipath on Orthogonal Chirp Division Multiplexing in Shallow Water Acoustic Channel

BAI YIQI[1] AND HE CHUANLIN[1,2]
[1]Institute of Oceanographic Instrumentation, Shandong Academy of Sciences, Qilu University of Technology, Qingdao 266100, China
[2]School of Ocean Science, Shandong Academy of Science, Qilu University of Technology, Qingdao 266100, China

Corresponding author: Bai Yiqi (baiyiqi817@outlook.com)

ABSTRACT In the scenario of underwater acoustic communication, Orthogonal Frequency Division Multiplexing (OFDM) is widely used for its high spectral efficiency and high transmission rate. However, OFDM is sensitive to Doppler shift, which will generate inter-carrier interference to degrade bit error rate performance. Orthogonal Chirp Division Multiplexing (OCDM) consists of multiplexing a number of chirp waveforms that are mutually orthogonal with each other and share the same bandwidth and time slot, achieving good robustness against multipath and Doppler shift. This study reviews the concepts of Orthogonal Chirp Division Multiplexing and combines this multicarrier communication scheme with an underwater acoustic channel. Unlike previous studies analyzing within the signal domain, this study formulates the mathematical model of OCDM in shallow water acoustic channel and illustrates the reason why OCDM can outperform OFDM in both Doppler robustness and multipath robustness, which is a necessary and solid complement for OCDM in the further development of underwater acoustic communication.

INDEX TERMS Orthogonal chirp division multiplexing, shallow water acoustic channel, under water acoustic communication.

I. INTRODUCTION

The underwater acoustic channel is considered one of the most difficult wireless communication channels for multipath transmission, time variation, limited bandwidth, and Doppler shift [1]. Especially for shallow water acoustic channel, the above-mentioned characteristics make signal vary severely in time and selective fading in the frequency domain [2]. In order to achieve a high transmission rate and high Underwater Acoustic Communication (UAC) system performance, the design of the system should balance spectrum efficiency and robustness [3].

At present, high-speed UAC systems employing single-carrier and multi-carrier modulation techniques have been widely examined [4]. Orthogonal Frequency Division Multiplexing (OFDM) is a multi-carrier modulation method that is extensively applied in UAC system for high spectrum efficiency, low computational complexity, and easily equipped with Fast Fourier Transform [5]. In the application of underwater acoustic communication, lots of OFDM-based techniques such as channel coding [6], channel estimation [7], time synchronization [8], and Doppler compensation [9] are investigated in the last decades. Therefore, high-speed OFDM in UAC is boosted in the aspect of communication distance as well as communication robustness [10]. However, the performance of OFDM in UAC is limited by the sensitivity to Doppler shift, which will destroy the orthogonality of the sub-carriers. As a result, an inter-carrier interference (ICI) compensation algorithm such as Doppler shift correction is usually required, which will add to the complexity of the OFDM system [11], [12]. On the other hand, the Linear Frequency Modulation (LFM) signal is resistant to

The associate editor coordinating the review of this manuscript and approving it for publication was Jiajia Jiang.

B. Yiqi, H. Chuanlin: Analysis of Doppler and Multipath on Orthogonal Chirp Division Multiplexing in Shallow Water Acoustic Channel

IEEE *Access*

the detrimental effects of shallow water acoustic channel. By modulating information via a broad spectrum LFM signal, Chirp Spread Spectrum (CSS) modulation technique offers robust performance with a simple matched filtering-based decoder, which can achieve high processing gain as well as high multipath resolution [13]. Therefore, CSS is very attractive for a low data rate UWAC system when reliability is considered a priority factor.

Recently, a novel technique termed Orthogonal Chirp Division Multiplexing (OCDM) has been proposed for coherent optical communication system [14]. OCDM consists of multiplexing a number of chirp waveforms that are mutually orthogonal with each other and share the same bandwidth and time slot, achieving good robustness against multipath and Doppler shift [15]. The essence of OCDM is substituting sensitive sub-carriers in OFDM for insensitive sub-carriers(i.e. LFM) [16]. Additionally, OCDM can achieve better performance with a similar peak-to-average power ratio and spectral efficiency compared with OFDM [17]. Up to now, OCDM is widely used in optical fiber communication [18], [19], transferometric power line sensing [20], and underwater acoustic communication [21]. In reference [21], a UAC system based on OCDM is proposed and the system performance on an under-loaded scenario is investigated which shows a promising bit error rate (BER) compared to traditional OFDM. Up to now, the research of OCDM in UAC is mainly focused on channel equalization algorithms [22], [23], [24] and extending OCDM to MIMO system [25]. However, the above-mentioned results are described with respect to the signal domain and lack quantitative analysis on Doppler and multipath effects when introducing OCDM to the SWAC model. The purpose of this paper is to study the Doppler and multipath resistance of the OCDM system, which is a necessary and solid complement for OCDM application in the further development of underwater acoustic communication.

The structure of this paper is organized as follows: section 2 describes the OCDM principles whereas section 3 presents the Doppler and multipath analysis of OCDM in SWAC. In section 4, the performance results of both OCDM and OFDM systems over a static and dynamic channel are provided. Finally, the conclusions are summarized in section 5.

II. PRINCIPLES OF OCDM
A. OCDM BASIS
Similar to OFDM based on Fourier Transform, the principles of OCDM originated from the Fresnel Transform, which is an important transform in the Linear Canonical Transform (LCT). The kernel of OCDM modulation is based on a set of orthogonal chirp signals while mutually overlapping in the time domain and the frequency domain. Define the quadratic exponential waveforms $\psi_n(t)$ with chirp wave-number $n \in [0, N-1]$ temporally limited on symbol duration T_u, such as:

$$\psi_n(t) = e^{\frac{\pi}{4}} e^{-j\pi \frac{N}{T_u^2}\left(t - n\frac{T_u}{N}\right)^2} \quad 0 \leq t < T_u \quad (1)$$
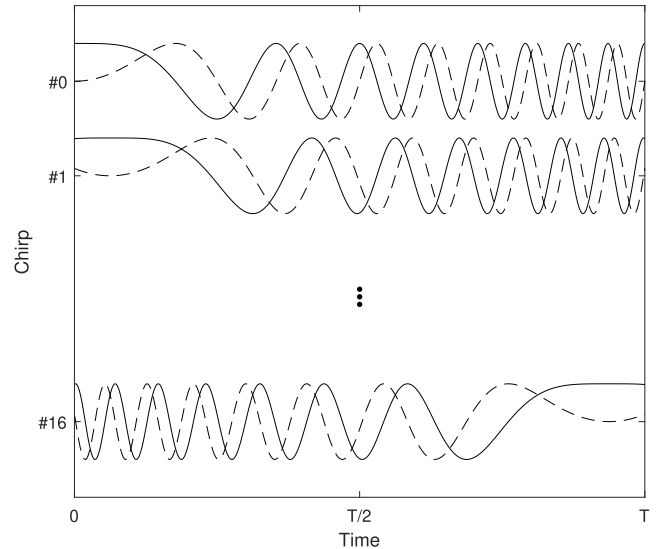

FIGURE 1. OCDM chirp waveforms for N=16.

As an example, a 16-chirped OCDM system is illustrated in Fig. 1, where the real part of chirped waveforms is depicted in a solid line, whereas the dashed line stands for the imaginary part. It is obvious that these sets of chirp waves share the same chirp rate $\alpha = N/T_u^2$ leading to a bandwidth $B = N/T_u$. The sub-carriers of the OCDM multi-carrier modulation system are mutually orthogonal in the chirp domain, which can be easily verified as follows:

$$\int_0^{T_u} \psi_m^*(t)\psi_n(t)\,dt$$

$$= \int_0^{T_u} e^{j\pi \frac{N}{T_u^2}\left(t - m\frac{T_u}{N}\right)^2} e^{-j\pi \frac{N}{T_u^2}\left(t - n\frac{T_u}{N}\right)^2}\,dt$$

$$= \begin{cases} 1 & \text{if m=n} \\ 0 & \text{instead} \end{cases} \quad (2)$$

Similar to OFDM, both amplitude and phase information can be modulated. In the time domain, the baseband transmission signal for the OCDM block k labeled as $s_k(t)$ can be obtained by multiplexing these N waveforms over the duration T. This set of waveform is multiplied by a quadrature amplitude modulation (QAM) cell x_k^n that carrying the useful information:

$$s_k(t) = \sum_{n=0}^{N-1} x_k^n \psi_n(t), \quad t \in [0, T_u] \quad (3)$$

In underwater acoustic communication, there exist severe multipath propagation in the wireless channel, especially in shallow water acoustic channel. In order to prevent inter-symbol interference (ISI), a cyclic prefix (CP) with time scale T_{CP} is added at the beginning of each OCDM block signal. The time duration T_{CP} should cover the delay spread of the current channel, which prolongs the baseband

transmission signal as follows:

$$\underline{s_k}(t) = \begin{cases} s_k(t + T_u - T_{CP}) & 0 \le t < T_{CP} \\ s_k(t - T_{CP}) & T_{CP} \le t < T \\ 0 & \text{else} \end{cases} \quad (4)$$

The total time duration of the OCDM baseband transmission signal is $T = T_u + T_{CP}$, therefore, K OCDM symbols can be written as:

$$s(t) = \sum_{k=0}^{K-1} \underline{s_k}(t - kT) \quad (5)$$

In the demodulation part of OCDM, utilizing the orthogonal properties of OCDM sub-carrier $\psi_n(t)$ concluded from (2), the transmission data $\hat{x}_k^n$ can be achieved by applying match filter to received signal $r(t)$:

$$\hat{x}_k^n = \int_0^{T_u} r(t - kT + T_{CP}) \psi_n^*(t)\, dt \quad (6)$$

B. OCDM IN DIGITAL STRUCTURE

Equations (3) and (4) realize the analog signals for OCDM, the digital signal of OCDM modulation is performed by using inverse discrete Fresnel transform (IDFnT), as shown in [26]. In fact, sampling (3) at mT_u/N yields:

$$s_m^k = s_k(t)_{t=m\frac{T_u}{N}} = \sum_{n=0}^{N-1} x_n^k \psi_n(mT_u/N)$$

$$= e^{j\frac{\pi}{4}} \sum_{n=0}^{N-1} x_n^k e^{-j\frac{\pi}{N}(m-n)^2} \quad (7)$$

From the above expression, the concise matrix form of OCDM modulation can be expressed as:

$$\mathbf{s} = \mathbf{\Phi}^H \mathbf{x} \quad (8)$$

with $\mathbf{s} = [s_{1,k} \cdots s_{N,k}]^T$, $\mathbf{x} = [x_{1,k} \cdots x_{N,k}]^T$ and unitary DFnT matrix $\mathbf{\Phi} \in C^{N \times N}$ defined as follows:

$$\{\mathbf{\Phi}\}_{m,n} = \frac{1}{\sqrt{N}} e^{-j\frac{\pi}{4}} e^{j\frac{\pi}{N}(m-n)^2} \quad (9)$$

As a result, the baseband OCDM signal $\mathbf{s}$ with loaded data $\mathbf{x}$ is achieved by DFnT matrix $\mathbf{\Phi}$. However, the process of demodulating signals with DFnT/IDFnT requires excessive computational complexity $(\approx O(N^2))$ that cannot be rapidly deployed to offshore devices such as buoys. In order to reduce the computational complexity, in [15], the authors present a compensation matrix to implement DFnT/IDFnT with discrete Fourier transform $(\approx O(N \log_2^N))$. Thus, the OCDM demodulation can be realized from the following expression by an existing OFDM system without an increase of complexity.

$$\mathbf{y} = \mathbf{F} \cdot \mathbf{r} = \mathbf{\Gamma}^H \mathbf{\Lambda} \mathbf{F} \mathbf{x} + \mathbf{w} \quad (10)$$

where $\mathbf{F}$ is the Fourier matrix of size N, $\mathbf{\Gamma}$ and $\mathbf{\Lambda}$ are both diagonal matrices of size $N \times N$. In the case of N being even:

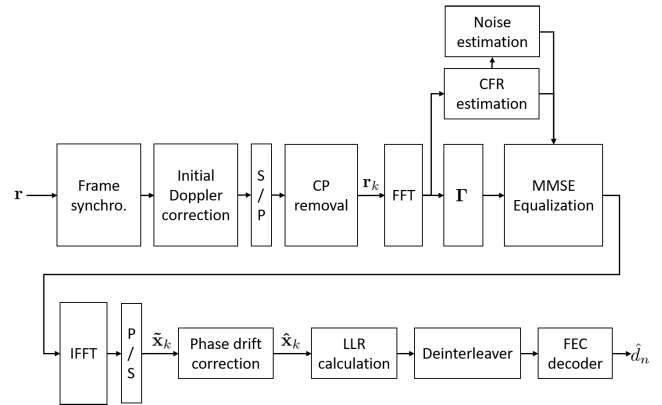$$\mathbf{\Gamma}_{n,n} = e^{-j\frac{\pi}{N}n^2} \quad (11)$$

FIGURE 2. OCDM decoder structure.

$$\mathbf{\Lambda}_{n,n} = H_n \quad (12)$$

In the above expressions, H_n is the channel frequency response (CFR) of the channel at the n-th frequency bin. Additionally, $\mathbf{w}$ is the noise vector assumed Gaussian with zero mean and variance noted σ_w^2. From the above-mentioned procedure, the decoder structure of OCDM with MMSE channel estimation and soft decision algorithm can be summarized as Fig. 2.

To illustrate the differences between the presented OCDM and traditional OFDM, the comparison will elaborate as follows:

. The complementation of OCDM is based on the Discrete Fresnel Transform and OFDM is based on Discrete Fourier Transform.
. The waveform of sub-carriers in OCDM is the LFM signal(wideband signal, modulated in both time and frequency domain) while OFDM is a single frequency signal(modulated in frequency domain).
. The computational complexity of OCDM is $O(N^2)$, whereas that of OFDM is $O(N \log_2^N)$
. The modulation/demodulation process of OCDM can be achieved in the time domain while OFDM is achieved in the frequency domain.

III. ANALYSIS OF OCDM IN SHALLOW WATER ACOUSTIC CHANNEL

As known that the underwater acoustic channel is most challenging due to its double dispersion property in both long time delay and large Doppler spread, resulting in the severe multipath spread and time variation, especially for the SWAC [27]. Since the OCDM communication system is a typical wideband system, where Doppler shifts each frequency component by a different amount. Here, a more generalized channel model(i.e., uniform path speed model) is applied to formulate the transmission of OCDM signals in SWAC.

In the uniform path speed model, a constant relative speed between the transmitter and receiver is assumed by the dominant arrival path. Additionally, a Doppler expansion is

utilized with the same ratio which leads to the same scaling ratio while the absolute Doppler spread may differ from different frequencies. Therefore, the following context will be categorized into the following two parts: Doppler analysis and multipath analysis of OCDM in SWAC.

A. DOPPLER ANALYSIS OF OCDM IN SWAC

In shallow water acoustic channel, the determinant Doppler originated from uniform relative speed is far larger than the random speed from current, ocean surface fluctuation, floating matters in the water column, etc. Therefore, the uniform relative speed will be primarily considered in the paper. Introduced from the uniform path speed model, the channel between transmission signal $s(t)$ and received signal $r(t)$ can be expressed as follows:

$$r(t) = as[D(t - \tau(t))] \tag{13}$$

where the channel exists a constant Doppler i.e. radial velocity v, a represents amplitude factor, $D = c/(c+v)$ is the scaling factor from Doppler, and $\tau(t)$ is the time delay. Substituting equation 1 into the above expression, the received signal of the OCDM sub-carrier is thus:

$$r_n(t) = ae^{-j\pi \frac{N}{T_u^2}\left((Dt)^2 - 2nD\frac{T_u}{N}t\right)} e^{j\phi_n} \tag{14}$$

with $\phi_n = -\pi \left(N/T_u^2\right) \cdot (nT_u/N)^2 = -\pi n^2/N$ is the phase related to wave-number. Compared between equation 1(without Doppler) and equation 14(with Doppler), it can be concluded that the Doppler changes chirp rate from N/T_u^2 to $D^2 N/T_u^2$ as well as changes center frequency from $2nT_u/N$ to $2nDT_u/N$. In a realistic underwater acoustic communication scenario, the Doppler scaling factor D remains very close to 1 with large velocity(i.e., $D \approx 0.996$ when relative radial velocity equals 10 m/s). Therefore, the following expressions assume that the Doppler only exists on the changes of the center frequency. For simplicity, the phase related to the sub-carrier will not be involved.

$$r_n(t) = ae^{-j\pi \frac{N}{T_u^2}\left(t^2 - 2n(D-1)\frac{T_u}{N}t + 2n\frac{T_u}{N}t\right)} e^{j\phi_n}$$
$$= ae^{j\left(\frac{1}{2}\mu t^2 + \omega_0 t + \omega_d t\right)} \tag{15}$$

where $\mu = 2N\pi/T_u^2$ is the chirp rate of the chirp signal and $\omega_d = 2n\pi(D-1)/T_u$ is the frequency shift due to Doppler. Convert above expression into frequency domain:

$$R_n(\omega) = a \int_{\frac{T_u}{2}}^{\frac{T_u}{2}} e^{j\left[(\omega_0 + \omega_d - \omega)t + \frac{1}{2}\mu t^2\right]} dt$$
$$= a \int_{\frac{T_u}{2}}^{\frac{T_u}{2}} e^{j\frac{\mu}{2}\left[\left(t - \frac{\omega - \omega_0 - \omega_d}{\mu}\right)^2 - \left(\frac{\omega - \omega_d - \omega_d}{\mu}\right)^2\right]} dt \tag{16}$$

Utilizing changing the upper and lower limits bond of the integration as well as the symmetric property of Fresnel integration, substitute $\frac{\pi}{2}x^2 = \frac{\mu}{2}\left(t - \frac{\omega - \omega_0 - \omega_d}{\mu}\right)$ in (16):

$$R_n(\omega) = a\sqrt{\frac{\pi}{\mu}} e^{\frac{-j}{2\mu}(\omega - \omega_0 - \omega_d)^2} \int_{-v_1}^{v_2} e^{i\pi \frac{x^2}{2}} dx$$

$$= a\sqrt{\frac{\pi}{\mu}} e^{\frac{-j}{2\mu}(\omega - \omega_0 - \omega_d)^2}$$
$$\cdot \left[\int_{-v_1}^{v_2} \cos\left(\frac{\pi}{2}x^2\right) dx + i \int_{-v_1}^{v_2} \sin\left(\frac{\pi}{2}x^2\right) dx\right] \tag{17}$$

where the upper and lower limit of the integration can be written as:

$$v_1 = \frac{-\mu T/2 - (\omega - \omega_0 - \omega_d)}{\sqrt{\pi \mu}}$$
$$v_2 = \frac{\mu T/2 - (\omega - \omega_0 - \omega_d)}{\sqrt{\pi \mu}} \tag{18}$$

Expand the brackets in (17) for the further details:

$$[\ ] = \int_0^{v_2} \cos\left(\frac{\pi}{2}x^2\right) dx - \int_0^{-v_1} \cos\left(\frac{\pi}{2}x^2\right) dx$$
$$+ i\left[\int_0^{v_2} \sin\left(\frac{\pi}{2}x^2\right) dx - \int_0^{-v_1} \sin\left(\frac{\pi}{2}x^2\right) dx\right]$$
$$= c(v_2) - c(-v_1) + i[s(v_2) - s(-v_1)] \tag{19}$$

It is obvious that both $c(v)$ and $s(v)$ are Fresnel integration:

$$c(v) = \int_0^v \cos\left(\frac{\pi}{2}x^2\right) dx$$
$$s(v) = \int_0^v \sin\left(\frac{\pi}{2}x^2\right) dx \tag{20}$$

According to the odd symmetry property of Fresnel integration(i.e., $c(v) = -c(-v)$ and $s(v) = -s(-v)$), substitute (19) into (17):

$$R_n(\omega) = a\sqrt{\frac{\pi}{\mu}} e^{\frac{-j}{2\mu}(\omega - \omega_0 - \omega_d)^2}$$
$$\cdot \{[c(v_1) + c(v_2)] + i[s(v_1) + s(v_2)]\}$$
$$= a\sqrt{\frac{\pi}{\mu}} e^{\frac{-j}{2\mu}(\omega - \omega_0 - \omega_d)^2 + \arctan\frac{s(v_1) + s(v_2)}{c(v_1) + c(v_2)}}$$
$$\cdot \left\{[c(v_1) + c(v_2)]^2 + i[s(v_1) + s(v_2)]^2\right\}^{\frac{1}{2}} \tag{21}$$

Reminding that the OCDM is a combination of LFM signals, the product of time duration and signal bandwidth BT is far beyond 1 in most circumstances. According to the mathematical inference in the previous article [28], [29], The OCDM signal with Doppler shift in the frequency domain can be achieved as follows:

$$R_n(\omega) = a\sqrt{\frac{2\pi}{\mu}} e^{j\left[\frac{(\omega - \omega_0 - \omega_d)^2}{2\mu} + \frac{\pi}{4}\right]} \tag{22}$$

On the other hand, the frequency response of a Linear Frequency Modulation signal with ideal match filter can be referred as $H(\omega) = exp^{[j((\omega - \omega_0)^2/2\mu - \omega t_d + \pi/4)]}$, where t_d is the time delay of match filter. Therefore, the result of received OCDM signal after ideal match filter can be written as:

$$Y_n(\omega) = R_n(\omega) H(\omega)$$
$$= a\sqrt{\frac{2\pi}{\mu}} e^{j\left[\frac{(2\omega - 2\omega_0 - \omega_d)\omega_d}{2\mu} - \omega t_d\right]} \tag{23}$$

Convert $Y_n(\omega)$ in time domain:

$$y_n(t) = \frac{1}{2\pi} \int_{-\infty}^{\infty} Y_n(\omega) e^{j\omega t} d\omega$$

$$= aT_u \sqrt{\frac{\mu}{2\pi}} \frac{\sin\left[\mu T_u \left(t - t_d + \frac{\omega_d}{\mu}\right)/2\right]}{\mu T_u \left(t - t_d + \frac{\omega_d}{\mu}\right)/2} e^{j\omega_0(t - t_d)}$$

(24)

The envelope of the non-Doppler(i.e. $\omega_d = 0$) match filter can be expressed as:

$$\underline{y_n}(t) = aT_u \sqrt{\frac{\mu}{2\pi}} \frac{\sin\left[\mu T_u (t - t_d)/2\right]}{\mu T_u (t - t_d)/2}$$

(25)

Comparing between (24) and (25), it can be concluded that the existence of Doppler shifts introduce a time shift $t_d' = \omega_d/\mu = 2\pi(D-1)/\mu T_u$ to the envelope of match filter time domain result, which is irrelevant to the wave-number of OCDM sub-carrier. Therefore, all sub-carriers share the same time shift t_d', where the orthogonal property of OCDM remains stable and no inter-carrier interference introduces to OCDM signal.

In the following simulation, a Doppler estimation sequence is deployed at the beginning of the OCDM signal. Doppler compensation can be proceeded from signal compression rate or expansion rate by mentioned Doppler estimation sequence and no residual Doppler remains, which is difficult to compensate in OFDM. It can be concluded that OCDM decreases the complexity of Doppler estimation and compensation of underwater acoustic communication system.

B. MULTIPATH ANALYSIS OF OCDM IN SWAC

According to the uniform path speed model, the multi-path channel without Doppler as follows:

$$h(t, \tau) = \sum_{l=1}^{L} a_l(t) \delta(t - \tau_l(\tau))$$

(26)

where L is the amount of multipath(i.e., the number of channel taps), $a_l(t)$ is the amplitude factor of l-th channel tap, and $\tau_l(t)$ is the time delay of l-th channel tap. In the scenario of shallow water multi-carrier acoustic communication, the center frequency is high enough to assume amplitude remains constant in a single frame. Substitute (1) into (26):

$$r(t) = \sum_{l=1}^{L} a_l \frac{1}{\sqrt{N}} \sum_{n=0}^{N-1} x_n e^{j\pi \frac{N}{T_u^2}\left(t - t_l - n\frac{T_u}{N}\right)^2} + n(t)$$

(27)

Thus, the demodulation result from (2) can be written:

$$\hat{x}_m = \int r(t) \psi_m^* dt$$

$$= \int \sum_{l=1}^{L} a_l \sum_{n=0}^{N-1} x_n e^{j\pi \frac{N}{T_u^2}\left(t - t_l - n\frac{T_u}{N}\right)^2} e^{-j\pi \frac{N}{T_u^2}\left(t - m\frac{T_u}{N}\right)^2} dt$$

$$= \int \sum_{l=1}^{L} a_1 x_n e^{j2\pi \frac{m-n}{T_u} t} dt$$

$$+ \int \sum_{l=2}^{L} a_l \sum_{n=0}^{N-1} x_n e^{-j2\pi \frac{N}{T_u^2}\left(t - n\frac{T_u}{N}\right)\tau_l} e^{-j\pi \frac{(m^2 - n^2)}{N}} e^{j\theta_l} dt$$

(28)

In the above expression, the first item represents the direct arrival component, which contains the desired data for the following demodulation process. The second item is the multipath interference(i.e., ISI), which involves three parts: ICI term $exp\left(-j\pi\left(m^2 - n^2\right)/N\right)$, an exponential term $exp\left(-j2\pi\left(N/T_u^2\right)(t - nT_u/N)\tau_l\right)$, and $\theta_l = \pi\tau_l^2 N/T_u^2$ related to multipath delay τ_l.

In the case of $m = n$(i.e., ICI free), desired data $\hat{x}_m$ can be estimated from m-th direct arrival component. Where $m \neq n$, the summation in the second term over sub-carriers attenuates as sinc function for a specific time delay τ_l. Moreover, the ICI term and exponential term introduce additional decay of multipath interference according to the channel delay τ_l. Therefore, OCDM can achieve better SNR performance for the above-mentioned attenuation on multipath component, while multipath interference accumulates at sub-carrier frequencies in OFDM.

IV. SIMULATION OF OCDM IN SWAC

In this section, the underwater acoustic communication system with OCDM is simulated over Watermark BCH1 channel. The BCH1 channel implements a replayed channel simulator driven by at-sea measurements of the time-varying CIR. As shown in Fig. 3, the BCH1 channel is located at the commercial harbor of Brest, France. TX is the source hydrophone and RX is a 4-element array lowered into the water column. A single probe transmission over a range of 800 m resulted in a 59.4 s channel estimate, simultaneously recorded on the four hydrophones [30].

The water depth of the BCH1 channel is around 20 m, which is a typical shallow water acoustic channel. Meanwhile, BCH1 channel is considered an ideal channel for multipath simulation because the water column in the harbor is relatively stable leading to a small Doppler shift around -1
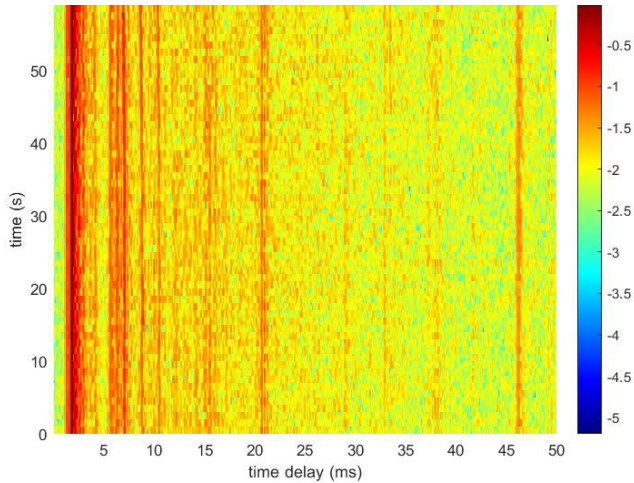
B. Yiqi, H. Chuanlin: Analysis of Doppler and Multipath on Orthogonal Chirp Division Multiplexing in Shallow Water Acoustic Channel

IEEE Access

FIGURE 4. The CIR variation profile of BCH1 shallow water acoustic channel.
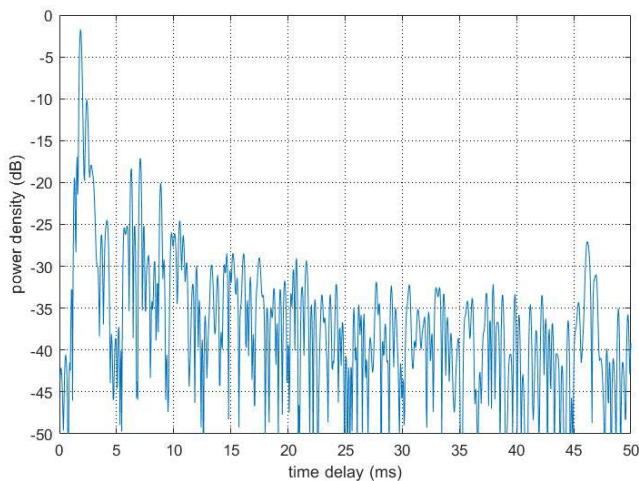
FIGURE 5. The power delay profile of BCH1 shallow water acoustic channel.

TABLE 1. Parameters of the BCH1 simulation.

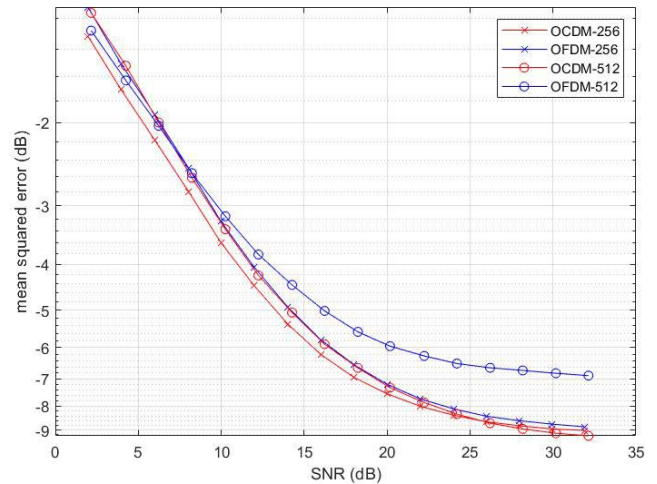|		
f_c	Center carrier frequency	35 kHz
f_s	Sample frequency in passband	100 kHz
B	Bandwidth for bseeband signal	4 kHz
M	Constellation order	4 (QPSK)
g_f	Fec coder	$(117, 134)_o$
R_c	FEC rate	1/2 (LDPC)
N	Number of waveforms	256 / 512
N_d	Number of data blocks per frame	3
R_{CP}	Cyclic prefix ratio	0.25
T_g	Guard interval time	256 ms
T_f	Frame time length	576ms/896ms

FIGURE 6. BCH1 Simulation results of mean squared error with estimated SNR in multipath scenario.
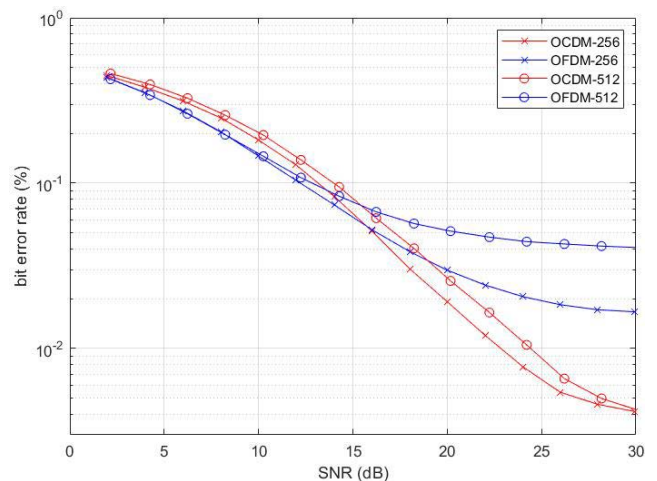

FIGURE 7. BCH1 Simulation results of bit error rate with estimated SNR in multipath scenario.

to 1 Hz. In the case of Doppler simulation, a fixed Doppler shift or a uniform Doppler scale factor can be easily imported. The CIR of channel is shown in Fig. 4 and Fig. 5.

The CIR of channel is shown in Fig. 4 and Fig. 5. It can be concluded that the dominant arrival carries most of the energy and the energy of the following echos with different time delay decay exponentially. The difference between direct arrival and the first echo reaches around 20dB. Therefore, the BCH1 channel is a classic shallow water acoustic channel with lots of multipath components and small variations in time. The simulation parameters are listed in Table. 1.

In the case of multipath scenario, the performances of MSE and BER are plotted respectively in Fig. 6 and Fig. 7. It can be concluded that OCDM provided a MSE enhancement compared with OFDM on the BCH1 channel in the multipath scenario. In Fig. 6, in the low SNR region, OCDM and OFDM have the same MSE, however, in the high SNR region, OCDM can achieve better performance than OFDM. In other

words, OCDM can achieve the same MSE as OFDM with lower SNR (around 6 dB SNR enhancement when MSE = −6 dB).

This MSE gain is logically converted to BER enhancement, as shown in Fig. 7. The SNR enhancement in OCDM remains 6 dB corresponding to MSE result. Additionally, one can note that the BER gain is getting higher as the number of
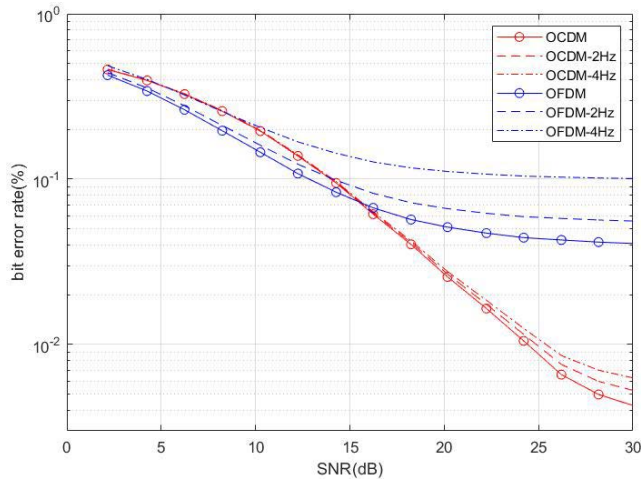
FIGURE 8. BER results of BCH1 shallow water acoustic channel in Doppler scenario.
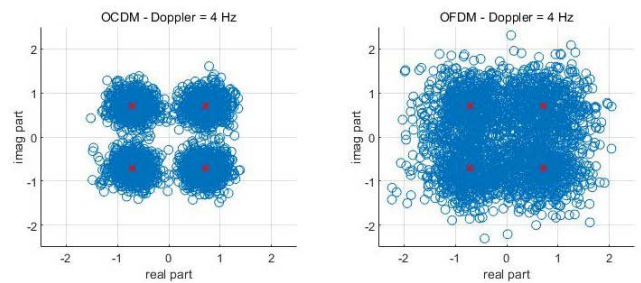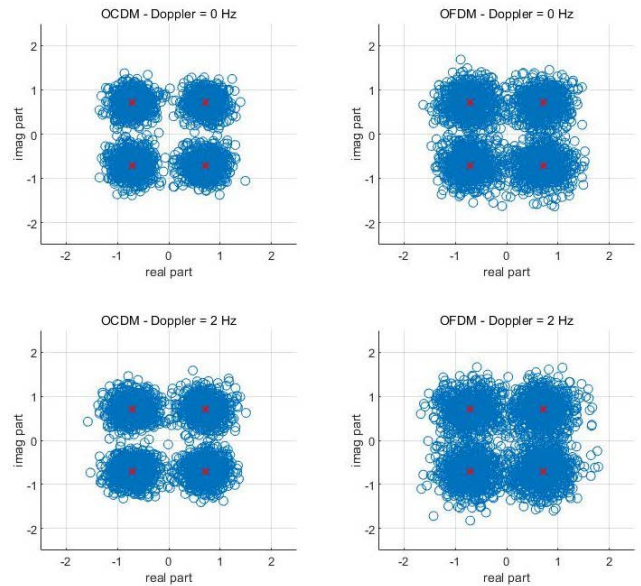

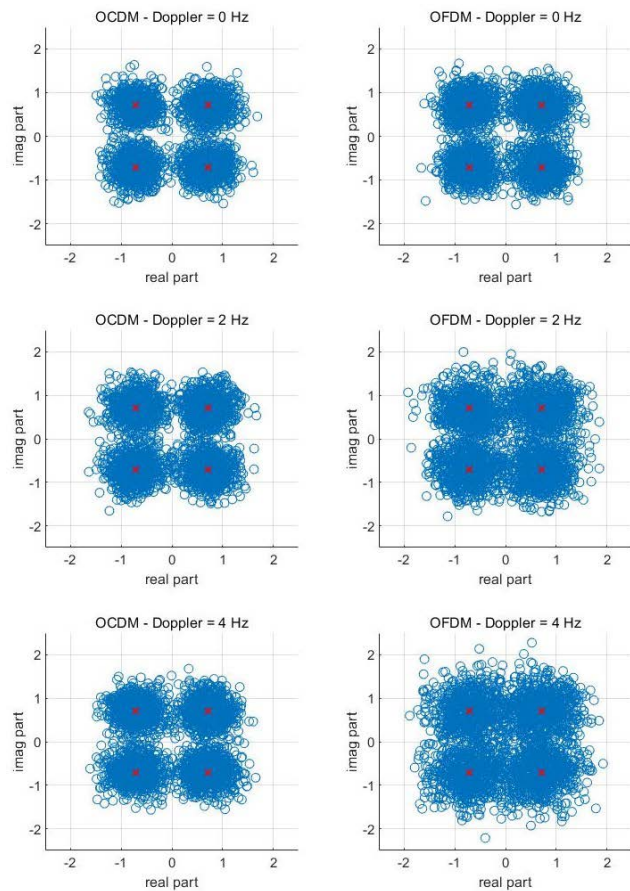**FIGURE 9.** Constellation Plot for OCDM and OFDM with SNR=15dB.

FIGURE 10. Constellation Plot for OCDM and OFDM with SNR=25dB.

In the case of the Doppler scenario, different Doppler shifts are introduced manually in the signal receiving part. The performance of BER is plotted in Fig. 8. Compared with the result in multipath scenario(i.e. no Doppler shift), it can be inferred that with the increase of Doppler shift, BER performance of both OCDM and OFDM are decreasing, while OCDM can maintain a relatively low BER below 10^{-2}. With different Doppler shifts, OCDM remains strong robustness against Doppler, while OFDM diverges with the increasing Doppler shift. OCDM outperforms OFDM in the tolerance of Doppler shift, which can be verified by (25).

Fig. 9 and Fig. 10 are the constellation scatter figures under SNR=15 dB and SNR=25 dB respectively, with the increasing Doppler shift, the decoded data from OCDM shows the consensus stability. Meanwhile, the decoded data from OFDM diverges along with the increasing Doppler shifts, which is corresponding to Fig. 8. It can be concluded from the above-mentioned figures that the OCDM can achieve better BER performance in high SNR conditions, where the SNR enhancement is around 6 to 7 dB.

V. CONCLUSION

In shallow water acoustics communication, OCDM has been proved as a reliable approach for its high spectrum efficiency as well as Doppler and multi-path robustness. In this paper, the combination of OCDM and shallow water acoustic

sub-carriers N decreases. This phenomenon demonstrates that OCDM can achieve better robustness from multipath echos for the energy is interfered with each other. On the contrary, the interference is superimposing in the OFDM situation.

B. Yiqi, H. Chuanlin: Analysis of Doppler and Multipath on Orthogonal Chirp Division Multiplexing in Shallow Water Acoustic Channel

IEEE *Access*

uniform path speed channel model is formulated leading to the analysis on both Doppler and multipath of OCDM. With respect to Doppler, the orthogonal property of OCDM remains stable and no inter-carrier interference introduces to the OCDM signal for all sub-carriers in OCDM sharing the same time shift. Meanwhile, the multipath interference component in OCDM attenuates instead of accumulating at sub-carrier frequencies in OFDM. Based on the Water-Mark simulation, the data from BCH1 channel demonstrates that OCDM can boost the decoding SNR and significantly enhance the decoding performance. The SNR enhancement can achieve 6 to 7 dB at SNR=25 dB and BER reaches below 10^{-2} at 4Hz Doppler shift.

REFERENCES

[1] M. C. Domingo, "Overview of channel models for underwater wireless communication networks," *Phys. Commun.*, vol. 1, no. 3, pp. 163–182, 2008.

[2] M. Stojanovic, "Underwater acoustic communication," in *Wiley Encyclopedia of Electrical and Electronics Engineering*. 1999, pp. 1–12.

[3] Z. Lv, Y. Bai, J. Jin, H. Wang, and C. Ren, "Analysis of wave fluctuation on underwater acoustic communication based USV," *Appl. Acoust.*, vol. 175, Apr. 2021, Art. no. 107820.

[4] M. Y. I. Zia, J. Poncela, and P. Otero, "State-of-the-art underwater acoustic communication modems: Classifications, analyses and design challenges," *Wireless Pers. Commun.*, vol. 116, no. 2, pp. 1325–1360, Jan. 2021.

[5] G. Avrashi, A. Amar, and I. Cohen, "Time-varying carrier frequency offset estimation in OFDM underwater acoustic communication," *Signal Process.*, vol. 190, Jan. 2022, Art. no. 108299.

[6] L. Wan, H. Zhou, X. Xu, Y. Huang, S. Zhou, Z. Shi, and J.-H. Cui, "Adaptive modulation and coding for underwater acoustic OFDM," *IEEE J. Ocean. Eng.*, vol. 40, no. 2, pp. 327–336, Apr. 2014.

[7] M. Stojanovic, "OFDM for underwater acoustic communications: Adaptive synchronization and sparse channel estimation," in *Proc. IEEE Int. Conf. Acoust., Speech Signal Process.*, Mar. 2008, pp. 5288–5291.

[8] W. Wei, H. Xiaoyi, W. Deqing, X. Ru, and S. Haixin, "Performance comparison of time synchronization algorithms for OFDM underwater communication system," in *Proc. 14th Int. Conf. Mechatronics Mach. Vis. Pract.*, Dec. 2007, pp. 104–107.

[9] A. E. Abdelkareem, B. S. Sharif, and C. C. Tsimenidis, "Adaptive time varying Doppler shift compensation algorithm for OFDM-based underwater acoustic communication systems," *Ad Hoc Netw.*, vol. 45, pp. 104–119, Jul. 2016.

[10] G. Qiao, Z. Babar, L. Ma, S. Liu, and J. Wu, "MIMO-OFDM underwater acoustic communication systems—A review," *Phys. Commun.*, vol. 23, pp. 56–64, Jun. 2017.

[11] B. Li, F. Tong, J.-H. Li, and S.-Y. Zheng, "Cross-correlation quasi-gradient Doppler estimation for underwater acoustic OFDM mobile communications," *Appl. Acoust.*, vol. 190, Mar. 2022, Art. no. 108640.

[12] A. E. Abdelkareem, B. S. Sharif, C. C. Tsimenidis, and J. A. Neasham, "Time varying Doppler-shift compensation for OFDM-based shallow underwater acoustic communication systems," in *Proc. IEEE 8th Int. Conf. Mobile Ad-Hoc Sensor Syst.*, Oct. 2011, pp. 885–891, doi: 10.1109/MASS.2011.105.

[13] L. Marchetti and R. Reggiannini, "An efficient receiver structure for sweep-spread-carrier underwater acoustic links," *IEEE J. Ocean. Eng.*, vol. 41, no. 2, pp. 440–449, Apr. 2016.

[14] X. Ouyang and J. Zhao, "Orthogonal chirp division multiplexing for coherent optical fiber communications," *J. Lightw. Technol.*, vol. 34, no. 18, pp. 4376–4386, Sep. 15, 2016.

[15] X. Ouyang and J. Zhao, "Orthogonal chirp division multiplexing," *IEEE Trans. Commun.*, vol. 64, no. 4, pp. 3946–3957, Sep. 2016.

[16] L. de M. B. A. Dib, G. R. Colen, M. de L. Filomeno, and M. V. Ribeiro, "Orthogonal chirp division multiplexing for baseband data communication systems," *IEEE Syst. J.*, vol. 14, no. 2, pp. 2164–2174, Jun. 2020.

[17] H. Attar, "Peak-to-average power ratio performance analysis for orthogonal chirp division multiplexing multicarrier systems based on discrete fractional cosine transform," *Int. J. Commun., Netw. Syst. Sci.*, vol. 9, no. 12, p. 545, 2016.

[18] F. Lu, L. Cheng, M. Xu, J. Wang, S. Shen, and G.-K. Chang, "Orthogonal chirp division multiplexing in millimeter-wave fiber-wireless integrated systems for enhanced mobile broadband and ultra-reliable communications," in *Proc. Opt. Fiber Commun. Conf.*, 2017, p. Th4E-5.

[19] X. Ouyang, G. Talli, and M. Power, "Orthogonal chirp-division multiplexing for IM/DD-based short-reach systems," *Opt. Exp.*, vol. 27, no. 16, pp. 23620–23632, 2019.

[20] L. Giroto de Oliveira, M. de Lima Filomeno, H. V. Poor, and M. V. Ribeiro, "Orthogonal chirp-division multiplexing for power line sensing via time-domain reflectometry," *IEEE Sensors J.*, vol. 21, no. 2, pp. 955–964, Jan. 2021.

[21] Y. Bai and P.-J. Bouvet, "Orthogonal chirp division multiplexing for underwater acoustic communication," *Sensors*, vol. 18, no. 11, p. 3815, Nov. 2018.

[22] R. Bomfin, M. Chafii, and G. Fettweis, "Low-complexity iterative receiver for orthogonal chirp division multiplexing," in *Proc. IEEE Wireless Commun. Netw. Conf. Workshop*, Apr. 2019, pp. 1–6.

[23] X. Wang, Z. Jiang, and X.-H. Shen, "Low complexity equalization of orthogonal chirp division multiplexing in doubly-selective channels," *Sensors*, vol. 20, no. 11, p. 3125, Jun. 2020.

[24] M. S. Omar and X. Ma, "Pilot symbol aided channel estimation for OCDM transmissions," *IEEE Commun. Lett.*, vol. 26, no. 1, pp. 163–166, Jan. 2022.

[25] B. Wang and X. Guan, "Channel estimation for underwater acoustic communications based on orthogonal chirp division multiplexing," *IEEE Signal Process. Lett.*, vol. 28, pp. 1883–1887, 2021.

[26] X. Ouyang, C. Antony, F. Gunning, H. Zhang, and Y. Liang Guan, "Discrete Fresnel transform and its circular convolution," 2015, *arXiv:1510.00574*.

[27] F. Qu, Z. Wang, L. Yang, and Z. Wu, "A journey toward modeling and resolving Doppler in underwater acoustic communications," *IEEE Commun. Mag.*, vol. 54, no. 2, pp. 49–55, Feb. 2016.

[28] R. J. Adams and B. A. Davis, "Fresnel integral equations," in *Proc. IEEE Antennas Propag. Soc. Int. Symp.*, vol. 1, Jun. 2003, pp. 649–652.

[29] Y. Z. Umul, "Equivalent functions for the Fresnel integral," *Opt. Exp.*, vol. 13, pp. 8482–8489, Oct. 2005.

[30] F. X. Socheleau, A. Pottier, and C. Laot, "Watermark: bch1 dataset description," *Appl. Acoust.*, Jun. 2012.

BAI YIQI was born in Handan, China, in 1992. He received the B.S. and M.S. degrees in ocean technology from the Ocean University of China, Qingdao, China, in 2016, where he received the Ph.D. degree in ocean acoustic technology, in 2021.

Since 2021, he has been a Research Assistant with the Ocean Acoustics Laboratory, Institute of Oceanographic Instrumentation, Shandong Academy of Science, Qilu University of Technology. His research interests include underwater acoustic communication, acoustic signal processing, and underwater acoustic survey.

HE CHUANLIN was born in Shandong, China. He received the B.S. degree in information countermeasure technology and the Ph.D. degree in underwater acoustics engineering from Northwestern Polytechnical University, Xi'an, in 2010 and 2017, respectively.

Since 2017, he has been an Associate Researcher with the Ocean Acoustics Laboratory, Institute of Oceanographic Instrumentation, Shandong Academy of Science, Qilu University of Technology. His research interests include underwater acoustic field analyse and underwater acoustic signal processing.

• • •